Steric Control of α- and β-Alkylation of Azulenone Intermediates in a Guanacastepene A Synthesis

ARTICLE *in* THE JOURNAL OF ORGANIC CHEMISTRY · FEBRUARY 2010

Impact Factor: 4.72 · DOI: 10.1021/jo902283a · Source: PubMed

6 AUTHORS, INCLUDING:

Karol Michalak
Comenius University in Bratislava
55 PUBLICATIONS **315** CITATIONS
SEE PROFILE

Michal Michalak
Polish Academy of Sciences
21 PUBLICATIONS **196** CITATIONS
SEE PROFILE

Gonzalo Jiménez-Osés
Universidad de La Rioja (Spain)
67 PUBLICATIONS **788** CITATIONS
SEE PROFILE

Jerzy Wicha
Polish Academy of Sciences
257 PUBLICATIONS **1,643** CITATIONS
SEE PROFILE

JOC Article
pubs.acs.org/joc

Steric Control of α- and β-Alkylation of Azulenone Intermediates in a Guanacastepene A Synthesis

Hao Wang,[†] Karol Michalak,[‡] Michał Michalak,[‡] Gonzalo Jiménez-Osés,[§] J. Wicha,[‡] and K. N. Houk*,[†]

[†]*Department of Chemistry and Biochemistry, University of California, Los Angeles, California 90095-1569,* [‡]*Institute of Organic Chemistry, Polish Academy of Sciences, ul. Kasprzaka 44/52, 01-224 Warsaw 42, Poland, and* [§]*Departamento de Química Orgánica y Química Física, CSIC-Universidad de Zaragoza, C/ Pedro Cerbuna, 12, E-50009 Zaragoza, Spain*

houk@chem.ucla.edu

Received October 26, 2009

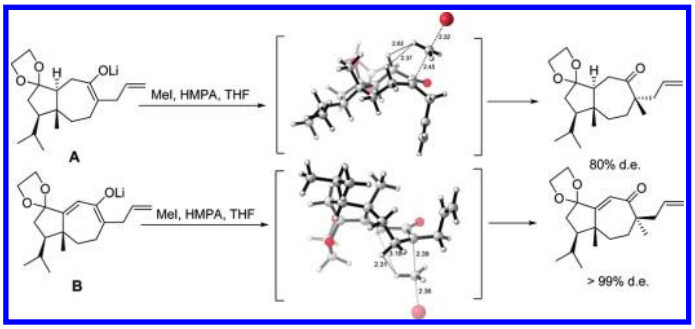

The origins of different stereoselectivities observed experimentally in the alkylations of azulenone precursors in the guanacastepene A synthesis have been determined through density functional theory investigations. The optimized transition structures of methylation of two different guanacastepene A precursors show that steric effects, rather than torsional factors that often determine such stereoselectivities, dictate the preferred products observed.

Introduction

The synthesis of stereochemically complex molecules requires control of the introduction of new stereogenic centers. The use of asymmetric catalysts to control the stereoselectivity of alkylations has been of much contemporary interest in this regard.[1] Although catalyst control can give high stereoselectivity, the modification of substrates to control stereoselective alkylations is also a venerable and useful strategy in synthesis. Understanding and predicting substrate-controlled stereoselective synthesis remains a challenging problem.[2] Stereoselective alkylations have been investigated by computational methods in a few cases,[3] and the role of torsional effects has been emphasized. Torsional effects control the trajectories of attack of electrophiles on electron-rich alkenes,[4] just as

(1) (a) Nicola, M. H.; Jeffrey, A. A.; Amir, H. H. *J. Am. Chem. Soc.* **1997**, *119*, 6205–6206. (b) He, X. X.; Lian, S. Z.; Wei, W. *J. Am. Chem. Soc.* **2007**, *129*, 10886–10894. (c) Denise, A.; Jonathan, A. *J. Am. Chem. Soc.* **2006**, *128*, 5604–5605. (d) Cristina, C.; Gianni, P.; Emanuela, V. *J. Org. Chem.* **2003**, *68*, 1200–1206. (e) Ivan, L. L.; Keunho, K.; Jin, K. C. *J. Am. Chem. Soc.* **2008**, *130*, 15997–16002.

(2) (a) Morris, W. J.; Shair, D. S. *Org. Lett.* **2009**, *11*, 9–12. (b) Takashi, E.; Toru, E.; Kazutaka, T.; Makoto, S. *J. Org. Chem.* **2006**, *71*, 8559–8564.

(3) (a) Soteras, I.; Lozano, O.; Escolano, C.; Orozco, M.; Amat, M.; Bosch, J.; Luque, F. J. *J. Org. Chem.* **2008**, *73*, 7756–7763. (b) Ando, K.; Green, N.; Li, Y.; Houk, K. N. *J. Am. Chem. Soc.* **1999**, *121*, 5334–5335. (c) Ikuta, Y.; Tomoda, S. *Org. Lett.* **2004**, *6*, 189–192. (d) Wu, Y.-D.; Houk, K. N.; Trost, B. M. *J. Am. Chem. Soc.* **1987**, *109*, 5560–5561. (e) Mukherjee, D.; Wu, Y.-D.; Fronczek, F. R.; Houk, K. N. *J. Am. Chem. Soc.* **1988**, *110*, 3328–3330. (f) Iafe, R. G.; Houk, K. N. *Org. Lett.* **2006**, *8*, 3469–3472. (g) Jimenez-Oses, G.; Aydillo, C.; Busto, J. H.; Zurbano, M. M.; Peregrina, J. M.; Avenoza, A. *J. Org. Chem.* **2007**, *72*, 5399–5402. (h) Ando, K. *J. Am. Chem. Soc.* **2005**, *127*, 3964–3972. (i) Soteras, I.; Lozano, O.; Gomez-Esque, A.; Escolano, C.; Orozco, M.; Amat, M.; Bosch, J.; Luque, F. J. *J. Am. Chem. Soc.* **2006**, *128*, 6581–6588. (j) Aydillo, C.; Jimenez-Oses, G.; Busto, J. H.; Zurbano, M. M.; Peregrina, J. M.; Avenoza, A. *Chem.—Eur. J.* **2007**, *13*, 4840–4848. (k) Kozlowski, M. C.; Dixon, S. L.; Panda, M.; Lauri, G. *J. Am. Chem. Soc.* **2003**, *125*, 6614–6615.

(4) (a) Caramella, P.; Rondan, N. G.; Paddon, M. N.; Houk, K. N. *J. Am. Chem. Soc.* **1981**, *103*, 2438–2440. (b) Rondan, N. G.; Paddon, M. N.; Caramella, P.; Mareda, J.; Mueller, P. H.; Houk, K. N. *J. Am. Chem. Soc.* **1982**, *104*, 4974–4976. (c) Paddon, M. N.; Rondan, M. N.; Houk, K. N. *J. Am. Chem. Soc.* **1982**, *104*, 7162–7166. (d) Lucero, M. J.; Houk, K. N. *J. Org. Chem.* **1998**, *63*, 6973–6977. (e) Cheong, P. H.; Yun, H.; Danishefsky, S. J.; Houk, K. N. *Org. Lett.* **2006**, *8*, 1513–1516. (f) Martinelli, M. J.; Peterson, B. C.; Khau, V. V.; Hutchinson, D. R.; Leanna, M. R.; Audia, J. E.; Droste, J. J.; Wu, Y.-D.; Houk, K. N. *J. Org. Chem.* **1994**, *59*, 2204–2210. (g) Lucero, M. J.; Houk, K. N. *J. Org. Chem.* **1998**, *63*, 6973–6977. (h) Houk, K. N.; Paddon-Row, M. N.; Rondan, N. G.; Wu, Y.-D.; Brown, F. K.; Spellmeyer, D. C.; Metz, J. T.; Li, Y.; Loncharich, R. J. *Science* **1986**, *231*, 1108–1117.

Published on Web 12/29/2009 DOI: 10.1021/jo902283a

SCHEME 1. Routes for the Alkylation of Two Different Hydroazulenone Intermediates

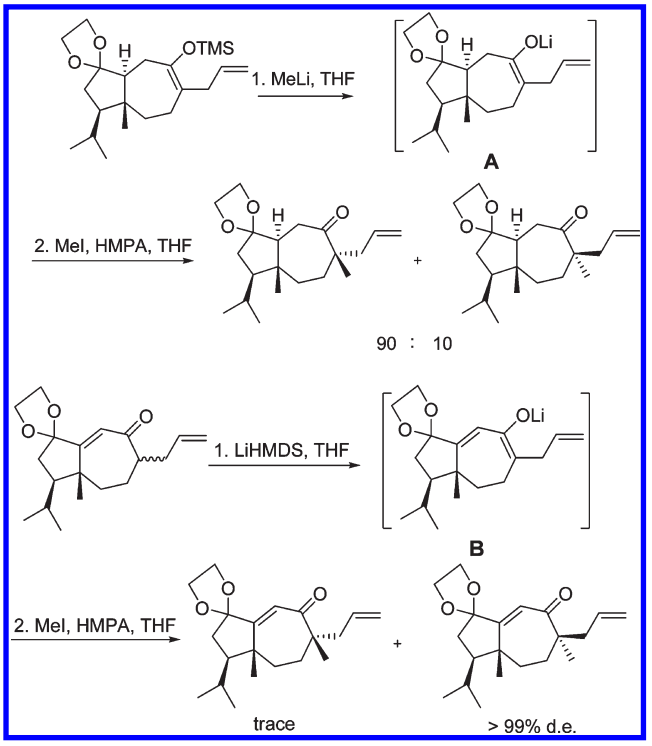

manifested for nucleophilic attack on carbonyls in the Felkin–Anh–Dunitz–Bürgi model.[5] Here we report a computational study that reveals that steric effects can sometimes override torsional effects, leading to different stereoselectivities in α- or *β*-alkylations of azulenone precursors in the guanacastepene A synthesis.

In recent attempts to complete the guanacastepene A total synthesis, opposite stereoselectivities were observed in the methylations of two rather similar azulenone intermediates (Scheme 1).[6] Enolate **A** gives the *β*-methylation product in 72% yield with 9:1 diastereomeric ratio. Enolate **B**, which has an additional double bond at the ring junction, affords the α-methylation product in 98% yield, exclusively. The methylation stereoselectivity observed for enolate **B** is consistent with the experimental results reported by Danishefsky and Mehta for a related intermediate.[7] In order to determine the origins of these different stereoselectivities, we explored these reactions computationally.

Results and Discussion

The energy-minimized geometry of enolate **A** shown in Figure 1 was obtained with the B3LYP/6-31G* method.[8,9] The cycloheptenolate ring adopts a chair conformation in the substrate, and the allyl group is rotated down with respect to the ring. The allyl group can adopt a variety of other conformations, and the other three minimized

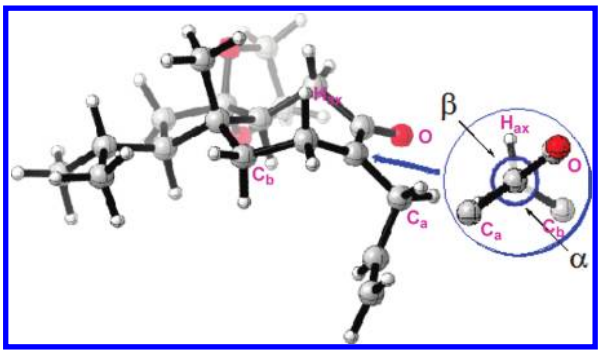

FIGURE 1. Lowest energy chairlike conformation of enolate **A**. A Newman projection viewed from the direction indicated by the blue arrow is also shown.

conformers are 0.5, 2.4, and 2.5 kcal/mol higher in energy, respectively (Supporting Information). The cycloheptenolate ring can also adopt a boat conformation in enolate **A**; however, the most stable boatlike conformation is less stable than the chairlike one by 1.6 kcal/mol. As shown in the Newman projection of enolate **A**, there is no difference between torsional effects for attack on the α or *β* face.

The alkylation transition states for the reaction of methyl bromide with enolate **A** were investigated next. Both chairlike and boatlike conformations of enolate **A** were considered in the transition states, and all different conformers with respect to the rotation of allyl and vinyl groups were explored (Supporting Information). For the alkylation on chairlike enolate **A**, six different *β*-attack transition state conformers were located with relative $\Delta\Delta G^{\ddagger}$ values of 0.0, 2.6, 2.7, 3.9, 4.4, and 5.6 kcal/mol, respectively. Six TS structures with $\Delta\Delta G^{\ddagger}$ values of 1.8, 4.2, 4.3, 5.8, 6.1, and 7.5 kcal/mol were found for the α-attack. The boatlike enolate **A** was also considered for the methylation transition states. The α-attack alkylation gave six transition state conformers with relative $\Delta\Delta G^{\ddagger}$ values of 2.4, 3.8, 4.3, 5.6, 5.7, and 5.8 kcal/mol, respectively. The *β*-attack transition state structures also gave six different conformers whose $\Delta\Delta G^{\ddagger}$ are 4.1, 5.7, 6.9, 8.1, 8.3, and 8.6 kcal/mol, respectively (Supporting Information).

From the energetics of the different transition state conformers, the most stable conformers of the transition states were located to be α/*β*-alkylation on chairlike enolate **A**. They are shown in Figure 2. The best α-methylation transition structure of enolate **A** (**1α**) is 1.8 kcal/mol higher energy than *β*-methylation transition state (**1*β***). This value was lowered to 1.1 kcal/mol by including solvation energies with the CPCM model[10] for methanol. (The solvent used experimentally was HMPA. No solvent model is available for HMPA, but methanol has a dielectric constant very similar to that of HMPA.) (Table 1) This value is consistent with the 1:9 α:*β* product ratios observed experimentally. Careful inspection of the two transition states suggests that the α-methylation transition state has no eclipsing (**1α′**), but there are significant repulsions between a methyl bromide H and two homoallylic Hs. They are separated by only 2.28 and 2.31 Å, less than the sum of their van der Waals radii (2.4 Å). However, there is only one H–H steric interaction

(5) Anh, N. T. *Top. Curr. Chem.* **1980**, *88*, 146–162.
(6) Michalak, K.; Michalak, M.; Wicha, J. Manuscript in preparation.
(7) (a) Mandal, M.; Yun, H. D.; Dudley, G. B.; Lin, S. N.; Tan, D. S.; Danishefsky, S. J. *J. Org. Chem.* **2005**, *70*, 10619–10637. (b) Mehta, G.; Umarye, J. D.; Srinivas, K. *Tetrahedron Lett.* **2003**, *44*, 4233–4237.
(8) Becke, A. D. *J. Chem. Phys.* **1993**, *98*, 5648–5652.
(9) Calculations were performed in Gaussian 03; Frisch, M. J. et al.; Gaussian Inc.: Pittsburgh, PA, 2004.
(10) (a) Barone, V.; Cossi, M. *J. Phys. Chem. A* **1998**, *102*, 1995–2001. (b) Cossi, M.; Rega, N.; Scalmani, G.; Barone, V. *J. Comput. Chem.* **2003**, *24*, 669–681.

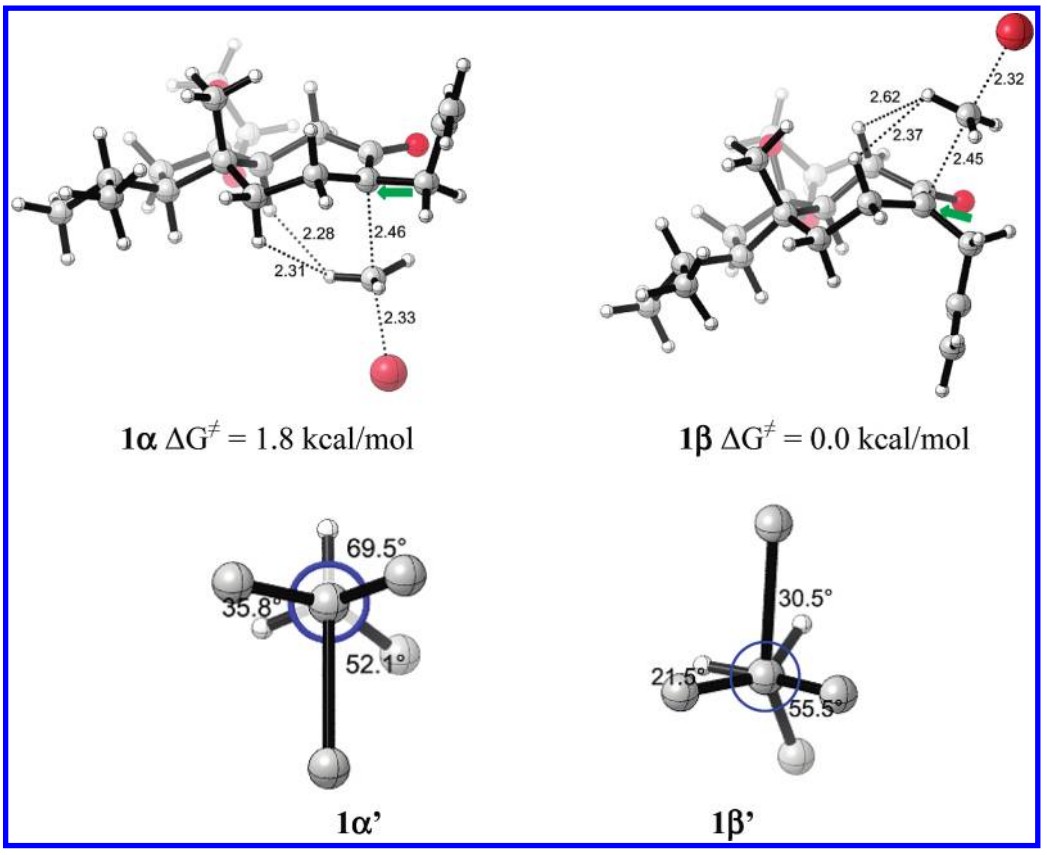

FIGURE 2. Transition structures for the α- and *β*-attack of methyl bromide on enolate **A**. Newman projections, **1α′** or **1*β*′**, are viewed from the directions indicated by the green arrows.

TABLE 1. Summary of Free Energies of 1α, 1*β*, 2α, and 2*β*

	G_{298} (gas)	G_{298} (solvent)[a]
$\Delta G^{\ddagger}$ (**1α**−**1*β***)	1.8 kcal/mol	1.1 kcal/mol
$\Delta G^{\ddagger}$ (**2*β***−**2α**)	5.2 kcal/mol	4.6 kcal/mol

[a]Solvent correction used the CPCM polarizable conductor calculation model as implemented in Gaussian 03. For **1α**, **1*β***, methanol was specified as the solvent (ε_{MeOH} = 32.6, while the experimental solvent is ε_{HMPA} = 30). For **2α**, **2*β***, THF was specified as the solvent.

(separated by 2.37 Å) in the *β*-attack transition structure, although there is some eclipsing between the forming bond and the axial CH bond (**1*β*′**).

Although torsional control of electrophilic or nucleophilic attack has been observed in a wide variety of situations,[4] it seems that the steric factors override the torsional effects in the stereoselective alkylations studied here. The two transition states are both staggered to a similar extent, but steric effects differentiate α and *β*-attack.

The geometry of enolate **B** was also optimized and is shown in Figure 3. In contrast with enolate **A**, the cycloheptadienolate ring adopts the twist-boat conformation in substrate **B**, and the allyl group is rotated up with respect to the ring. This conformer has literature precedent.[11] The energetically favorable twist-boat conformation of enolate **B** is more stable than the chair conformation as a result of the constraints of the additional double bond at the ring junction.[11b] The other three minimized conformers with respect to the rotation of allyl groups are 0.7, 1.8, and 2.3 kcal/mol

(11) (a) Crews, P. *Chem. Commun.* **1971**, 583–584. (b) Pearson, A. J.; Bansal, H. S. *Tetrahedron Lett.* **1986**, *27*, 287–290.

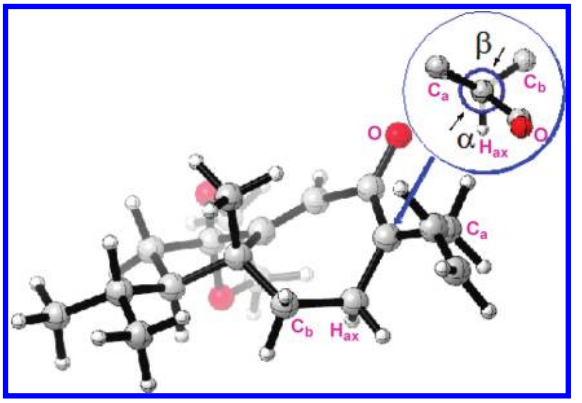

FIGURE 3. Lowest energy conformation of enolate **B.** The Newman projection is viewed from the direction indicated by the blue arrow.

higher in energy, respectively. As shown in the Newman projection of enolate **B**, there is no torsional difference for α or *β* attack.

Transition states of both α- and *β*-alkylation with methyl bromide on enolate **B** were then located, and all different rotamers with respect to the rotation of allyl and vinyl groups were considered (Supporting Information). Six different α-alkylation transition state conformers were obtained with relative $\Delta\Delta G^{\ddagger}$ values of 0.0, 1.3, 1.5, 2.5, 2.7, and 4.1 kcal/mol, respectively. For the *β*-alkylation transition states, another six different conformers were obtained whose $\Delta\Delta G^{\ddagger}$ are 5.2, 6.8, 7.6, 8.8, 9.1, and 9.9 kcal/mol with respect

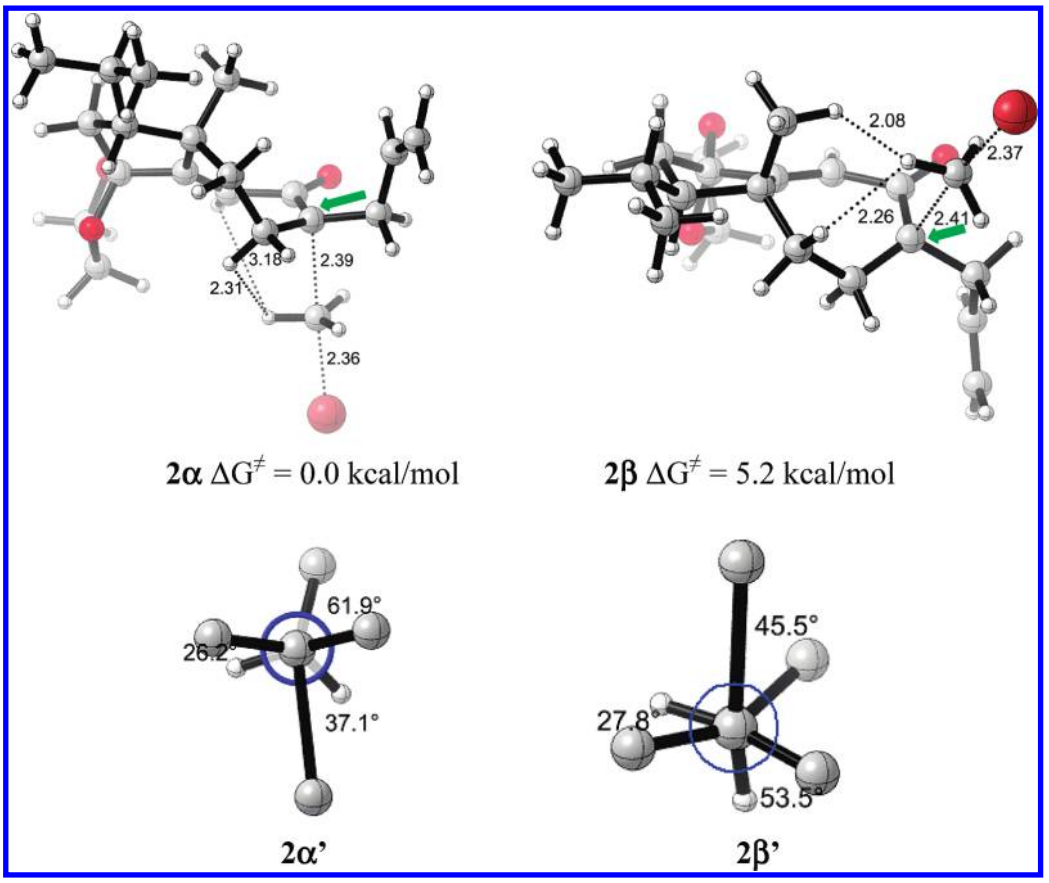

FIGURE 4. Transition structures for the α- and *β*-attack of methyl bromide on enolate **B**. Newman projections, **2α′** or **2*β*′**, are viewed from the directions indicated by the green arrows.

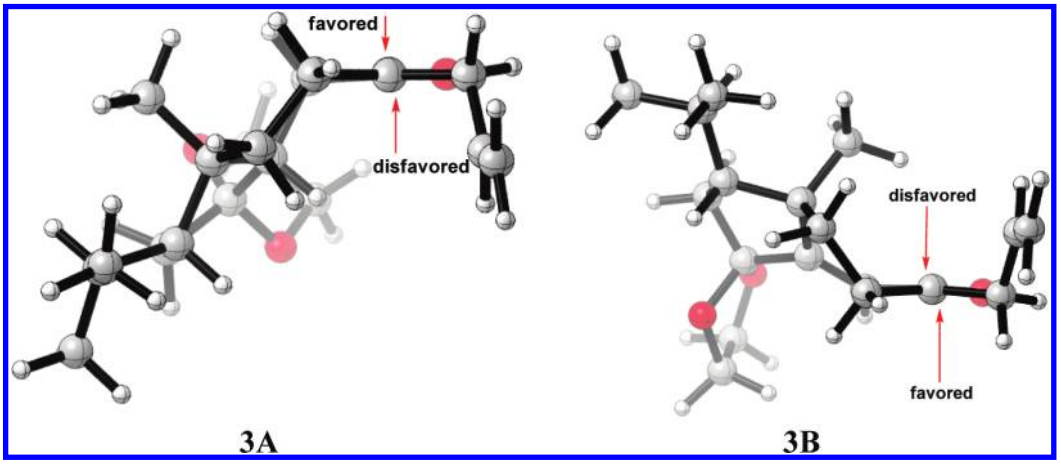

FIGURE 5. Optimized model reactants **A** and **B** looking along C=C.

to the lowest energy α-alkylation transition state. The most stable transition state conformers are shown in Figure 4. The α-methylation transition state (**2α**) is 5.2 kcal/mol more stable than the corresponding *β*-methylation transition state (**2*β***). This value is 4.6 kcal/mol when including solvation energies (Table 1, THF, CPCM model). This is in an excellent agreement with the experimental observation that methylation of enolate **B** takes place exclusively from the α-face. The large energy difference between the two transition structures is also due to steric factors rather than torsional effects. Both transition states have some torsional strain, shown in **2α′**, **2*β*′**. However, in contrast to the α-alkylation transition structure where only one H−H steric interaction exists (separated by 2.31 Å), *β*-alkylation process suffers significant steric repulsions between H on methyl bromide and two Hs on the substrate separated by 2.08 and 2.26 Å, respectively.

In fact, the qualitative origins of alkylation stereoselectivities can be identified from the geometry of the starting substrate (Figure 5).

As can be seen by inspection of the energetically favorable chair conformation of enolate **A** (**3A**), the α-face of the

cycloheptene ring is seriously blocked. Approach of the electrophile (CH_3I) is clearly preferred at the β-face for enolate **A**, which is consistent with the result obtained by TS exploration. With respect to enolate **B**, however, by adopting the twist-boat conformation, the left part of the cycloheptadienolate ring flips up (**3B**), which results in blocking the β-face toward attack and favoring the α-attack of the electrophile. The analysis of the geometries of the substrates again confirms that the stereoselectivities of alkylation result from steric effects. The allyl groups in **3A** and **3B** can adopt less hindered conformations, but the more rigid bicyclic groups dictate β and α attack, respectively.

In summary, the diastereoselectivities observed experimentally in azulenone enolates alkylation originate from the steric interactions between the alkylation reagent and the substrate. This investigation provides examples of steric effects controlling stereoselectivities with no torsional differentiation and provides guidance for the control of stereoselectivities by conformation manipulation of the substrates.

Acknowledgment. We are grateful to the National Institute of General Medical Sciences, National Institutes of Health for financial support of this research.

Supporting Information Available: Full computational details, Cartesian coordinates and energies of all reported structures, and imaginary frequencies of all transition states. This material is available free of charge via the Internet at http://pubs.acs.org.